Comparison of Electrical and Electromagnetic Properties of a Planar Inductor

Jurica Kundrata, Adrijan Barić
University of Zagreb, Faculty of Electrical Engineering and Computing
Unska 3, 10000 Zagreb, Croatia
E-mail: jurica.kundrata@fer.hr, adrijan.baric@fer.hr

***Abstract*— This paper compares the electromagnetic and electrical properties of a planar inductor used in a low-profile organic light-emitting diode (OLED) driver. A luminary consists of the OLED cell and its driver which uses a planar inductor. The proximity of the OLED cell and the constrained area makes the planar inductor lossy. The planar inductor represents a loop antenna and a main source of radiated emissions of the driver. The properties of the planar inductor are analysed w.r.t. the quality factor and the magnetic moment. The analysis uses a two-level experiment based on EM simulations to explore the geometrical parameters of the inductor. The experiment shows that the track width and the fill-ratio of the inductor have the largest effect on its properties. It is concluded that a planar inductor which introduces minimum power losses and radiated emissions to the OLED driver needs to be optimized w.r.t. the track width and the fill-ratio.**

***Keywords*—thick film inductor, electromagnetic modelling**

I. Introduction

Power converters utilize magnetic devices to store energy and low-profile applications use planar magnetic devices [1]. An example of a planar magnetic device which is commonly used in low-profile devices is the planar inductor [2]-[4].

Organic light-emitting diode (OLED) cells are planar, diffuse lighting devices and they form luminaries with a very low profile. The OLED luminary described in [5] drives the OLED cell using a buck converter. The buck converter utilizes a planar inductor which is considered lossy because of the proximity of the OLED cathode and the planar, distributed design. The planar inductor due to its inductive properties stabilizes the output current, while introducing power losses to the buck converter operation. Furthermore, the ripple of the output current of the buck converter causes the planar inductor to generate radiated emissions. The design of the planar inductor thus affects the operation of the buck converter and its radiated emissions.

The electrical properties of the planar inductor w.r.t. its geometrical design parameters is studied in [6]. A planar inductor on a printed circuit board (PCB) is used in a power converter and it is parametrized in [7]. The design of a planar inductor is optimized w.r.t. the power converter efficiency in [8] and a multiobjective optimization of the planar inductor is done in [9]. The electromagnetic compatibility (EMC) of the buck converters, i.e. its conducted emissions are studied in [10] and [11]. The radiated emissions of a power converter are considered w.r.t. the PCB layout in [12]. A buck converter which uses an air-core solenoid is characterized w.r.t. the magnetic field emissions in [13].

This work was supported by the European Commision under the Seventh Framework Programme (FP7) through project IMOLA „Intelligent light management for OLED on foil applications“ (Grant Agreement No. 288377).

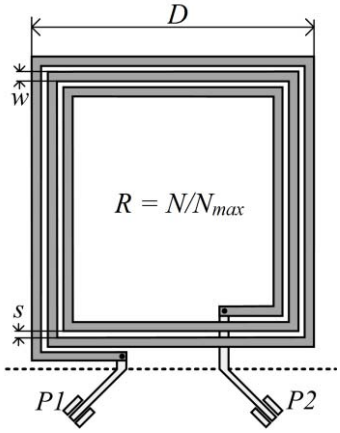

Figure 1. The design of the planar inductor and its parameters.

This paper compares the effects of the design parameters on the electrical properties of the planar inductor related to the buck converter and the radiated emissions of the planar inductor.

The analysis of the planar inductor is based on EM simulations described in Section II. The electrical properties of the planar inductor related to the buck converter are modelled in Section III, while Section IV presents the analysis of the radiated emissions of the planar inductor. The effects of the design parameters of the planar inductor on the electrical and electromagnetic properties are investigated using a screening experiment in Section V. The discussion of the experiment results is presented in Section VI, while Section VII contains the conclusions.

II. Electromagnetic Simulations

The planar inductor is a part of an OLED luminary which consists of the OLED cell and the backplane. The backplane contains the OLED driver, i.e. the buck converter that uses the planar inductor. The dimensions of the OLED cell limit the size of the backplane and thus the dimensions of the planar inductor.

This paper analyses a luminary which uses an OLED cell with dimensions 118x116 mm^2. The luminary is connected to a supply V_{IN} = 24 V and the buck converter supplies the OLED cell with the current I_{OUT} = 400 mA and the voltage V_{OUT} = 13.7 V. The buck converter operates at the switching frequency f_{SW} = 3.6 MHz.

Fig. 1 shows the layout of the planar inductor and its design parameters. The planar inductor has a square shape and its design is determined by the track width *w*, the track spacing *s*, the fill-ratio *R* and the outer dimension *D*. The fill-ratio *R* is the ratio of the number of turns *N* and the maximum number of turns which is determined by the pitch spacing *w+s* and the outer dimension *D*. The inductor structure has two ports *P1* and *P2*. The electrical properties of the planar inductor are simulated using COMSOL Multiphysics which result in two-port *S*-parameters [14].

The simulated substrate has two dielectric layers and three metal layers. The planar inductor is patterned on the 250 micron thick FR4 substrate and it uses two top metal layers which are made from 35 micron thick copper. The bottom metal layer represents the OLED cathode and the dielectric layer between the OLED cathode and the planar inductor represents the glass encapsulation.

The EM simulations analyse the frequency range 300 kHz to 300 MHz, which includes the switching frequency of the converter and the resonant behaviour of the inductor.

III. ELECTRICAL PROPERTIES

The electrical properties of the inductor are commonly represented by the quality factor *Q* which is defined at the frequency *f* as

$$Q(\mathrm{f}) = \frac{2\pi f L_S}{R_S} \tag{1}$$

where L_S is the series inductance and R_S is the series resistance of the inductor. The quality factor gives a ratio of the energy capacity of the inductor and its power losses.

The planar inductor stabilizes the output current of the buck converter, while introducing power losses in the conversion process. The stability of the output current is determined by the inductance, while the power losses are caused by the resistance of the planar inductor. The quality factor *Q* thus represents reasonable choice to represent the electrical characteristics of the planar inductor w.r.t. the buck converter.

The EM simulations of the planar inductor result in two-port *S*-parameters. The *S*-parameters are transformed to *y*-parameters which are used to define the interport, series admittance Y_3 by using

$$Y_3 = -\frac{y_{12} + y_{21}}{2}. \tag{2}$$

The series inductance L_S is extracted at the switching frequency by using

$$L_S = \mathrm{Im}\left[1/Y_3\right]/\left(2\pi f_{SW}\right) \tag{3}$$

and the series resistance R_S is extracted by using

$$R_S = \mathrm{Re}\left[1/Y_3\right]. \tag{4}$$

IV. ELECTROMAGNETIC PROPERTIES

The planar inductor consists of a number of turns and each turn acts as a loop antenna. The radiated emissions of the loop antenna are determined by its magnetic moment, i.e. the product of the loop area and current [15]. The magnetic moment *m* of the planar inductor is defined by the sum of the magnetic moments generated by the individual turns of the inductor which equals

$$m = \sum_{i=1}^{N} I_L A_{L,i} \tag{5}$$

where *N* is the number of turns of the planar inductor, I_L is the inductor current and $A_{L,i}$ is the area of the *i*-th inductor turn.

The current of the planar inductor I_L is determined by the ripple of the output current of the buck converter. The ripple current is related to the design parameters of the buck converter and the inductance of the planar inductor. The peak-to-peak value of the ripple current ΔI_{out} is defined as

$$\Delta I_{out} = \frac{V_{OUT}\left(V_{IN} - V_{OUT}\right)}{2\pi f_{SW} L_S V_{IN}}. \tag{6}$$

The magnetic moment of the planar inductor is derived by taking into account (6) and by determining the area of each inductor turn which leads to

$$m = \Delta I_{out} \sum_{i=1}^{N} \left[D - w - 2\left(i-1\right)\left(w+s\right)\right]^2. \tag{7}$$

V. GEOMETRICAL PARAMETER SCREENING

The geometrical design parameters of the planar inductor are screened by using a two-level full-factorial experiment [16]. Table 1 shows the levels of the design parameters used in the screening experiment. The planar inductor for each combination of the design parameters is simulated and the simulation results are used in determining the quality factor *Q* by using (1)-(4) and the magnetic moment *m* by using (6)-(7).

Fig. 2 shows the quality factor *Q* of the planar inductor w.r.t. the design parameters. Fig. 2 shows the relative value of the quality factor w.r.t. the two levels of the design

TABLE I
THE DESIGN PARAMETERS OF THE SCREENING EXPERIMENT.

Design parameter / Level	-1	+1
Track width *w* [mm]	0.2	0.5
Track spacing *s* [mm]	0.2	0.5
Fill-ratio *R* []	0.05	0.3
Outer dimension *D* [mm]	75	100

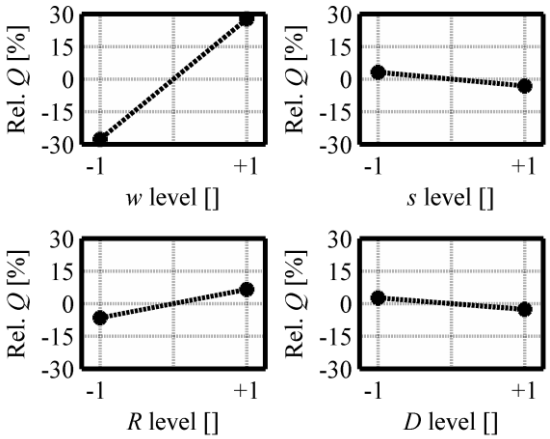

Figure 2. The quality factor Q w.r.t. the design parameters of the planar inductor.

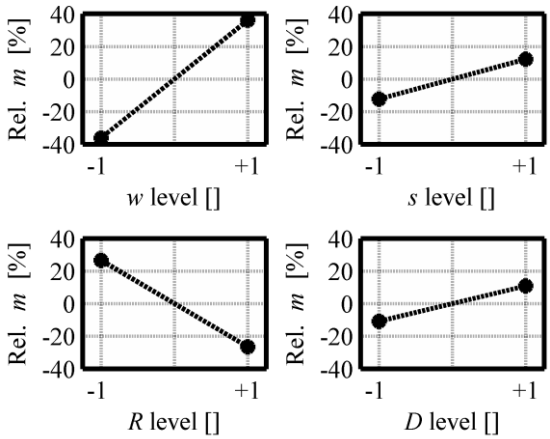

Figure 3. The magnetic moment m w.r.t. the design parameters of the planar inductor.

parameter. The results show that the track width w has the largest effect on the quality factor. It is observed that the effect of the fill-ratio R is relatively small, while the effects of the track spacing s and the outer dimension D on the quality factor are even smaller. The effects of the track width and the fill-ratio on the quality factor are positive, while the effects of the track spacing and the outer dimension are negative.

Fig. 3 shows the magnetic moment m of the planar inductor w.r.t. the design parameters. This figure shows the relative value of the magnetic moment w.r.t. the two levels of the design parameter. The results show that the track width w and the fill-ratio R have the largest effect on the magnetic moment. It is observed that the effects of the track spacing s and the outer dimension D on the magnetic moment are comparably smaller. The effects of the track width, the track spacing and the outer dimension on the magnetic moment are positive, while the effects of the fill-ratio are negative.

Table II shows the results of the analysis of variance (ANOVA) of the simulation results [17]. Table II shows the F-statistics and the p-value for the quality factor Q and the magnetic moment m w.r.t. the design parameters of the planar inductor. The results confirm the observations based on Figs. 2 and 3. The track width has the largest effect on the quality factor. The fill-ratio also has a notable effect, while the track spacing and the outer dimension have the comparably smallest effects on the quality factor. It is also confirmed that the track width and the fill-ratio have the largest effect on the magnetic moment.

VI. Discussion

Increasing the track width w reduces the resistance R_S of the inductor, while minimally influencing the inductance L_S of the inductor and thus the track width has a positive and a large effect on the quality factor Q.

The fill-ratio R determines the number of turns of the inductor. Increasing the fill ratio, i.e. the number of turns increases both the inductance L_S and the resistance R_S of the inductor. The results in Fig. 2 show that the inductance increase is larger than the resistance increase and thus the fill-ratio has a positive, notable effect on the quality factor Q.

The track spacing s influences the number of turns by modifying the track pitch. Increasing the track spacing while maintaining a fixed fill-ratio reduces the number of turns of the inductor. Due to the decrease in the number of turns, the inductance and the resistance of the inductor decrease as well. The inductance decrease is larger than the resistance decrease and thus the quality factor is reduced. The results on Fig. 2 show that this effect is indeed negative, but it is comparably smaller than the effects of the track width and the fill-ratio.

The outer dimension D influences the number of turns and the area of inductor. This influences the length of the inductor turns. These influences affect the inductance and the resistance of the inductor. The results show that these influences for the simulated parameter levels effectively cancel each other resulting in a very small, negative effect.

The magnetic moment m of the inductor is related to the ripple of the converter output current ΔI_{out}, i.e. the inductance L_S of the inductor. It is also related to the number of turns and the area of the inductor. Increasing the track width w while maintaining the fill-ratio R leads to a reduced number of turns. The reduced number of turns decreases the inductance of the inductor and consequently increases the ripple current of the buck converter. The results on Fig. 3 show that increasing the ripple current affects the magnetic moment much more than the decreased number of turns and results in a large, positive effect of the track width on the magnetic moment.

The fill-ratio R determines the number of turns and consequently influences the inductance of the inductor. Increasing the fill-ratio increases the inductance and thus reduces the current ripple. The results in Fig. 3 confirm that the inductance of the planar inductor has the largest effect on the magnetic moment and the fill-ratio has a large, negative effect on the magnetic moment.

Increasing the track spacing s reduces the number of turns and the inductance of the inductor. These changes

TABLE II
THE ANALYSIS OF VARIANCE OF THE SCREENING EXPERIMENT.

	Quality factor Q		Magnetic moment m	
	F	p-value [%]	F	p-value [%]
w	21.3	0.07	37.5	0.01
s	0.27	61.2	7.73	1.79
R	1.20	29.7	20.9	0.08
D	0.20	66.5	1.62	23.0

effectively cancel each other thus resulting in a comparably small, positive effect of the track spacing on the magnetic moment.

The outer dimension D directly influences the area of the inductor. Increasing the outer dimension increases the area and the inductance of the inductor. These changes effectively cancel each other thus resulting in a comparably small, positive effect of the outer dimension on the magnetic moment.

In summary, the results show that the track width w and the fill-ratio R have the largest influences on the quality factor Q and the magnetic moment m of the planar inductor. It is recommended to include these parameters in a co-optimization of the quality factor and the magnetic moment.

VII. Conclusions

A luminary consists of the OLED cell and its driver which uses a planar inductor. The planar inductor is the main source of radiated emissions of the driver. The properties of the planar inductor are analysed using EM simulations. The simulations are analysed w.r.t. the quality factor and the magnetic moment. The two-level screening experiment shows that the track width and the fill-ratio of the inductor have the largest effect on its properties. It is concluded that quality factor may be increased by increasing the track width of the inductor, while the magnetic moment is most sensitive to the changes in the inductance of the inductor.

References

[1] Z. Ouyang and M. Andersen, "Overview of planar magnetic technology; fundamental properties," *Power Electronics, IEEE Transactions on*, vol. 29, no. 9, pp. 4888–4900, Sept 2014.

[2] I. Kowase, T. Sato, K. Yamasawa, and Y. Miura, "A planar inductor using Mn-Zn ferrite/polyimide composite thick film for low-voltage and large current DC-DC converter," *Magnetics, IEEE Transactions on*, vol. 41, no. 10, pp. 3991–3993, Oct 2005.

[3] J.-J. Lee, Y.-K. Hong, S. Bae, J.-H. Park, J. Jalli, G. Abo, R. Syslo, B.-C. Choi, and G. Donohoe, "High-quality factor Ni-Zn ferrite planar inductor," *Magnetics, IEEE Transactions on*, vol. 46, no. 6, pp. 2417–2420, June 2010.

[4] Y. Yazaki, K. Ishidate, K. Hagita, Y. Kondo, S. Hattori, M. Sonehara, T. Sato, T. Watanabe, Y. Seino, and N. Matsushita, "Embedded planar power inductor in an organic interposer for package-level DC power grid," *Magnetics, IEEE Transactions on*, vol. 50, no. 11, pp. 1–4, Nov 2014.

[5] A. Monte, J. Doutreloigne, J. Windels, and P. Bauwens, "Driving electronics for OLED lighting," in *SID Mid-Europe Spring Meeting 2013*, 2013, pp. 12–15.

[6] J. Kundrata and A. Baric. "Design of a planar inductor for DC-DC converter on flexible foil applications," *MIPRO, 2012 Proceedings of the 35th International Convention*, pp. 54-59, May 2012.

[7] E. Waffenschmidt, B. Ackermann, and J. Ferreira, "Design method and material technologies for passives in printed circuit board embedded circuits," *Power Electronics, IEEE Transactions on*, vol. 20, no. 3, pp. 576–584, May 2005.

[8] C. Marxgut, J. Muhlethaler, F. Krismer, and J. Kolar, "Multiobjective optimization of ultraflat magnetic components with PCB-integrated core," *Power Electronics, IEEE Transactions on*, vol. 28, no. 7, pp. 3591–3602, July 2013.

[9] T. Andersen, C. Zingerli, F. Krismer, J. Kolar, N. Wang, and C. Mathuna, "Modeling and pareto optimization of microfabricated inductors for power supply on chip," *Power Electronics, IEEE Transactions on*, vol. 28, no. 9, pp. 4422–4430, Sept 2013.

[10] E. Rondon-Pinilla, F. Morel, C. Vollaire, and J.-L. Schanen, "Modeling of a buck converter with a SiC JFET to predict EMC conducted emissions," *Power Electronics, IEEE Transactions on*, vol. 29, no. 5, pp. 2246–2260, May 2014.

[11] C. Fuentes, B. Allongue, G. Blanchot, F. Faccio, S. Michelis, S. Orlandi, J. Pontt, J. Rodriguez, and M. Kayal, "Optimization of DC-DC converters for improved electromagnetic compatibility with high energy physics front-end electronics," *Nuclear Science, IEEE Transactions on*, vol. 58, no. 4, pp. 2024–2031, Aug 2011.

[12] A. Bhargava, D. Pommerenke, K. Kam, F. Centola, and C. W. Lam, "DC-DC buck converter EMI reduction using PCB layout modification," *Electromagnetic Compatibility, IEEE Transactions on*, vol. 53, no. 3, pp. 806–813, Aug 2011.

[13] S. Orlandi, B. Allongue, G. Blanchot, S. Buso, F. Faccio, C. Fuentes, M. Kayal, S. Michelis, and G. Spiazzi, "Optimization of shielded PCB air-core toroids for high-efficiency DC-DC converters," *Power Electronics, IEEE Transactions on*, vol. 26, no. 7, pp. 1837–1846, July 2011.

[14] *COMSOL Multiphysics 4.3 Users Guide*, 2012.

[15] D. Cheng, *Field and Wave Electromagnetics*. Addison-Wesley Longman, Inc., 1996.

[16] T. Santner, B. Williams, and W. Notz, *The Design and Analysis of Computer Experiments*. Springer, 2010.

[17] D. C. Montgomery, *Design and Analysis of Experiments*. John Wiley & Sons, 2008.